Plant Physiology and Biochemistry 165 (2021) 104–113

Contents lists available at ScienceDirect

Plant Physiology and Biochemistry

journal homepage: www.elsevier.com/locate/plaphy

Managing activity and Ca^{2+} dependence through mutation in the Junction of the AtCPK1 coordinates the salt tolerance in transgenic tobacco plants

G.N. Veremeichik *, Y.N. Shkryl, S.A. Silantieva, T.Y. Gorpenchenko, E.V. Brodovskaya, M. S. Yatsunskaya, V.P. Bulgakov

Federal Scientific Centre of the East Asia Terrestrial Biodiversity of the Far East Branch of the Russian Academy of Sciences, Vladivostok, 690022, Russia

ARTICLE INFO

Keywords:
Arabidopsis
Calcium-dependent protein kinases
Reactive oxygen species
Nicotiana tabacum
Salt tolerance
Heat shock factors

ABSTRACT

Calcium-dependent protein kinases (CDPKs) are Ca^{2+} decoders in plants. *AtCPK1* is a positive regulator in the plant response to biotic and abiotic stress. Inactivation of the autoinhibitory domain of AtCPK1 in the mutated form *KJM23* provides constitutive activity of the kinase. In the present study, we investigated the effect of overexpressed native and mutant *KJM23* forms on salinity tolerance in *Nicotiana tabacum*. Overexpression of native *AtCPK1* provided tobacco resistance to 120 mM NaCl during germination and 180 mM NaCl during long-term growth, while the resistance of plants increased to 240 mM NaCl during both phases of plant development when transformed with *KJM23*. Mutation in the junction KJM4, which disrupted Ca^{2+} induced activation, completely nullified the acquired salt tolerance up to levels of normal plants. Analysis by confocal microscopy showed that under high salinity conditions, overexpression of *AtCPK1* and *KJM23* inhibited reactive oxygen species (ROS) accumulation to levels observed in untreated plants. Quantitative real-time PCR analysis showed that overexpression of *AtCPK1* and *KJM23* was associated with changes in expression of genes encoding heat shock factors. In all cases, the KJM23 mutation enhanced the effect of AtCPK1, while the KJM4 mutation reduced it to the control level. We suggest that the autoinhibitory domains in CDPKs could be promising targets for manipulation in engineering salt-tolerant plants.

1. Introduction

Many physiological processes in living systems are controlled through a universal mechanism of calcium (Ca^{2+}) signalling (Bender et al., 2018). After an external stress stimulus, the cytosolic Ca^{2+} concentration ($[Ca^{2+}]$cyt) in the Ca^{2+} stores, extracellular and intracellular matrices, apoplast, and vacuole changes almost 10-fold within minutes (DeFalco et al., 2010; Kudla et al., 2010; McCarron et al., 2012). 'Ca2+ signatures' are a generally accepted hypothesis that complex spatio-temporal oscillations of $[Ca^{2+}]$cyt encode information for cellular responses (Edel and Kudla, 2015). One of the most important roles of calcium in plant physiology is the direct participation in salt tolerance (Manishankar et al., 2018). Salinity of soil, namely toxicity of Na^{+}, is an abiotic stress that can significantly reduce crop yield; therefore, investigations in this area are important (Sun et al., 2020). When the electrical conductivity of the soil is more than 4 dS m^{-1} (40 mM NaCl), it is considered saline; soil salinity can be as high as 2300 mM NaCl, while most crops can survive and produce fruits or seeds when growing in soils with no more 100 mM NaCl salinity (Manishankar et al., 2018). Supplementation with exogenous calcium in concentrations of 2–10 mM increased the salt tolerance of plants via regulation of ion homeostasis (Maeda et al., 2005; Manishankar et al., 2018; Tahjib-Ul-Arif et al., 2018).

Based on Ca^{2+} dependent regulation of salt-induced ROS production, it has been suggested that this secondary messenger plays a significant role in transpiration-dependent salt tolerance (Kudla et al., 2018). Ca^{2+} binding proteins translate the Ca^{2+} signal for a cell response. One group of Ca^{2+} decoders in plants is the calcium-dependent protein kinases (CDPKs) (Bender et al., 2018). Ca^{2+} ions at micromolar (1–5 μM) concentrations are sufficient for the function and activation of CDPKs (Bender et al., 2018). Since the first evidence of CDPKs' presence in plant cells (Harper et al., 1991; Watillon et al., 1993), *AtCPK1* (GenBank accession number, AT5G04870; http://www.uniprot.org/uniprot/Q06850) from *Arabidopsis* has become one of the most investigated members (Harper et al., 2004; Bender et al., 2018). Overexpression of *AtCPK1* led to an increase in drought and salt tolerance (Huang et al.,

* Corresponding author. Federal Scientific Centre of the East Asia Terrestrial Biodiversity FEB RAS, Vladivostok, 690022, Russia.
E-mail address: gala-vera@mail.ru (G.N. Veremeichik).

https://doi.org/10.1016/j.plaphy.2021.05.026
Received 4 April 2021; Accepted 17 May 2021
Available online 20 May 2021
0981-9428/

2017; Veremeichik et al., 2021) and phytoalexin biosynthesis (Shkryl et al., 2011, 2016; Veremeichik et al., 2016, 2019). Moreover, AtCPK1 regulates ROS production (Xing et al., 2001; Veremeichik et al., 2021) and can control cell death by phosphorylation of the main controller of cell death, ORE1 (Durian et al., 2020). These changes indicate that AtCPK1 plays an important role in the defence status of plant cells. This ability has attracted attention as a potential target for genetic boosting.

Generally, CDPK proteins consist of four domains: N-terminal, C-terminal Ca^{2+} binding, kinase and autoinhibitory domain. The N-terminal and C-terminal Ca^{2+} binding domain (CaM-like domain, CLD) activate the kinase domain PK (Harper et al., 2004). CLD is tethered to a PK via an autoinhibitory 35 a.a. junction (J) (Harmon et al., 1994; Hrabak et al., 2003), wherein the J and CLD domains do not function independently (Chandran et al., 2006) and form a single functional CDPK-activation domain (CAD) (Wernimont et al., 2011). The junction fragment of CAD occludes kinase activities when $[Ca^{2+}]$cyt is lease. Increasing $[Ca^{2+}]$cyt in response to external influences drives Ca^{2+} binding by CAD, and conformational changes removes the J fragment from the protein kinase active site. Free PK domains allow access to substrates (Bender et al., 2018).

Therefore, manipulations of CAD and the J fragment are the most prospective for genetic activation of CPK. Genetic removal of CAD from *Arabidopsis* CPK1 or CDPKα in soybean led to activation (Harper et al., 1994; Yoo and Harmon, 1996), but at the same time, a lack of CAD in another CPK, CPK17 from rice (an ortholog of *Arabidopsis* CPK1), led to the loss of catalytic activity *in vitro* (Almadanim et al., 2017). Moreover, inhibiting *Arabidopsis* CPK10 by EGTA suggested that a Ca^{2+} bound CAD may be important for CPK function (Boudsocq et al., 2012; Liu et al., 2016). Thus, point mutations in the junction are more suitable for genetic manipulation with CPK activation. One of the first and perhaps the most interesting scientific works in this area are the studies of Harper (1994) and Huang (1996). In these two works, several types of point mutations in J of AtCPK1 and truncated mutants (truncation of one of the CPK domain, including CAD) were analysed. The most active in the presence or absence of Ca^{2+} among point mutants and truncated mutants was mutant KJM23 (AV-424 to PD and QFSA-430 to PEDL in junction). Other types of mutations in J (KJM4, LRV-I444 to DLPG) were described by Huang et al. (1996). This mutation disrupted Ca^{2+} induced activation, which led to latent activity of KJM4 (Huang et al., 1996).

Among other Junction mutants in Harper's work, only KJM23-6H was the most active. KJM23 had a six amino acid substitution between residues A422 and A432. Its high activity compared to other compound mutations may indicate that partial autoinhibition can be obtained from non-homologous sequences located at the junction position (Harper et al., 1994). The KJM4 junction mutation completely abolished the binding of calmodulin. The C-terminus of the junction contains several overlapping sites (e.g., F436-I444 and F430-I444) that are analogous to the binding domains of calmodulin (Harmon et al., 1994; Harper et al., 1994; Huang et al., 1996). Interestingly, both types of the described substitutions altered the highly conserved amino acid residues of the CDPK junction domain. As previously described, the 35 a.a. Junction domain contains the subdomains of pseudosubstrate autoinhibition (from 17 to 26 a.a.) and CaMLD binding (from 23 to 35 a.a.) (Raichaudhuri et al., 2006). Four of the six amino acid residues of the KJM23 mutation replace the most constitutive residues of the pseudosubstrate autoinhibition subdomain (QFSA to PEDL), while the complete KJM4 mutation replaces the most constitutive residues of the CaMLD binding subdomain (LRVI to DLPG).

The effect of overexpression of the two mutant *AtCPK1* forms on plant cell physiology and biochemistry was analysed in comparison with the native form of *AtCPK1*. In our previous works, KJM23 and KJM4 were designated as *AtCPK1-Ca* (**C**onstitutively **a**ctive) and *AtCPK1-Na* (**N**ot **a**ctive), respectively. AtCPK1-Ca has been shown to be more effective than the native form in stimulating phytoalexin biosynthesis, such as that of anthraquinones, stilbenes, and isoflavonoids in transformed cell cultures of *Rubia cordifolia* L., *Vitis amurensis* Rupr., and *Glycine max* L., respectively (Shkryl et al., 2011, 2016; Veremeichik et al., 2016, 2019). Cultures transformed with *AtCPK1-Na* did not differ from the controls (Shkryl et al., 2011, 2016, 2016; Veremeichik et al., 2016). In the present work we used original terms, KJM23 for constitutively active mutant and KJM4 for not active mutant forms of AtCPK1.

Additionally, it has been shown that mutation KJM23 boosted the abilities of AtCPK1 to increase stress tolerance when mutation KJM4 nullified it (Veremeichik et al., 2021). However, these investigations were obtained on the atypical plant system (callus cultures of *R. cordifolia*) and need to be validated in whole plants. In our previous work (Veremeichik et al., 2021), we showed that native and Ca-mutant forms of *AtCPK1*-induced expression of ROS-scavenging enzymes, among others, had the highest expression of *RcApx2* (homolog of the *AtApx2*). Furthermore, stress inducible Apx2 is one of the target genes for heat stress transcriptional factors (TFs), HSFs (Guo et al., 2016). Plant HSFs regulate cell reactions to multiple abiotic stresses, including salinity. There are three subgroups of plant HSFs, called A, B, and C; HSFs from subgroup A function as transcription activators, and among them, HSFA1 (a, b, c, d, e) functions in stress response regulation (Huang et al., 2016). It is known, that expression of *AtHSFA1* is regulated through ROS induced Ca^{2+} signalling systems, and AtHSFA1 upregulates *AtHSFA2* and *AtHSFA3* expression and downregulates the expression of ABA-induced AtHSFA6b (Huang et al., 2016).

The aim of the present study was to validate two hypotheses: i) KJM23-mutations in the junction of AtCPK1 increase salt-stress tolerance in plants; and ii) KJM4-mutation turns off recombinant AtCPK1. To perform analyses, we used transgenic tobacco plants (*Nicotiana tabacum* L. var Xanthi nc). It is widely cultivated in many countries as one of the main industrial crops, therefore, research on the salt tolerance of tobacco is relevant and in demand (Sun et al., 2020). Beside these, tobacco is one of the most comfortable plants for transgene analysis due to the simplicity of tobacco transformation and plant regeneration (Horsch et al., 1985). In the present work, we analysed ROS accumulation and expression of the main *HSFs* in normal and *AtCPK1*-expressed tobacco plants at the earlier stages of salt stress and impact of two types of mutations in the Junction of *AtCPK1* on the transgene effect.

2. Materials and methods

2.1. Transformation of tobacco

Clonally cultivated plantlets of *Nicotiana tabacum* L. (cv Xanthi) were used for agrobacterium mediated transformation as described previously (Shkryl et al., 2018)). Leaf discs of sterile tobacco plantlets were inoculated with *Agrobacterium tumefaciens* carrying pART27/AtCPK1-KJM23 (active form), pART27/AtCPK1-KJM4 (non-active form) plasmids (Harper et al., 1994; Shkryl et al., 2011) and pPZP-RCS2-nptII/Ak (native form) plasmid (Shkryl et al., 2016). After 48 h co-cultivation with *A. tumefaciens* explants were transferred to the MS agarized medium (Murashige and Skoog, 1962) with 2 mg/L indole-3-butyric acid containing 100 mg/L kanamycine and 500 mg/L cefotaxime. Month-old primary calli was placing on hormone-free MS agarized medium containing 100 mg/L kanamycine under 16/8 h light/dark cycle for achieving of plant regeneration. Regenerated plantlets were rooted in MS/2 agarized medium (10 g/L sucrose) containing 100 and 200 mg/L kanamycine. Thus, transgenic plantlets expressing the selectable marker (*nptII*) gene together with the CPK1 (native), KJM23 (constitutively active), and KJM4 (non-active) forms of *AtCPK1* gene, namely CPK1-OE, KJM23-OE, and KJM4-OE, respectively, were obtained. The control non-transformed plants were established from the same plantlets and cultivated under the same conditions as the transformed ones (without antibiotics).

2.2. Detection and expression analysis of the AtCPK1 transcripts in transgenic tobacco plants and analysis of HSF genes expression

Isolation of total DNA, total RNA and first-strand cDNA synthesis were performed as described previously (Veremeichik et al., 2019). The primers 5′-TGT CTG GAG TGC TGG AGT GAT TGT G-3′ and 5′-TAG TCT ATT CGC CCG TCA TTG TCT T-3′ were used for PCR amplification of a 517 bp *AtCPK1* transcript (GenBank accession no. L14771) flanked mutations. As reference gene for Real Time PCR analysis of the *AtCPK1* gene expression we used *N. tabacum Actin* gene (GenBank accession no. XM_016609967) primers pair 5′- CTC CAA GCA GCA TGA AGA TTA AG -3′ and 5′- GAC TCG TCG TAC TCT GCC TTT G -3′ flanked 134 bp transcript and 242 bp product from DNA, with 108 bp intron. The fragments of the predicted length obtained in the PCR reactions with these primers and the cDNA from the regenerated plantlets *N. tabacum* were isolated from gels with a Glass Milk Kit (Sileks M) and subcloned into a pJET plasmid, using the ClonJet PCR Cloning Kit (ThermoFisher, USA). The clones were amplified with M13 universal primers and sequenced for confirmation of the mutation type in the *AtCPK1* gene in corresponding regenerated plantlets *N. tabacum* as described previously (Shkryl et al., 2008) at the Instrumental Centre of Biotechnology and Gene Engineering of FSCEATB FEB RAS using an ABI 3130 Genetic Analyzer (Applied Biosystems, Foster City CA, USA).

PCR and Real Time PCR reactions were done as described previously (Veremeichik et al., 2019) in a 10 μl volume containing 300 nM of each primer, 1 μl of the diluted cDNA sample and 2.5 mM $MgCl_2$ under the following conditions: 3 min at 96 °C, followed by 35 cycles of 15 s at 96 °C and 30 s at 60 °C in a 96-well reaction plate. For analysis two biological replicates were used and three technical replicates were analysed for each biological replicate. To verify the absence of contamination no-template controls and RNA-RT controls were included in the qPCR analysis. To confirmation the absence of non-specific products or primer–dimer artefacts in the samples we used melting curve analysis at the end of each run and product visualization using electrophoresis on a 1% agarose gel stained with ethidium bromide. Data were analysed using CFX Manager Software (Version 1.5; Bio-Rad Laboratories Inc., Hercules, CA).

For analysis of *NtHSF* genes expression we selected (using uniprot.com tools) the closest homologous to the main class A *HSFs* of *A. thaliana*: *NtHSFA1* (GeneBank № XP_016489250, homolog to *AtHSFA1* GeneBank № AP008209), *NtHSFA2* (GeneBank № LC427218, homolog to *AtHSFA2* GeneBank № AK118744), *NtHSFA3* (GeneBank № XM_016618411, homolog to *AtHSFA3* GeneBank № AK117318) *NtHSFA6b* (GeneBank № XP_016434163, homolog to *AtHSFA6b* GeneBank № NP_188922.1). For real time PCR we used primers pairs for *NtHSFA1*, 5′-GGA TTC TTC AGT TGG AGT AG-3′ and 5′-CTT TTT GAT TGT TTG ATG TTA GT-3′, for *NtHSFA2* 5′-GAC CCC CAG TAG TGA GAA TC-3′ and 5′-CTT CCT CTG CTC CAT CCC C-3′, for *NtHSFA3*,5′-GTG CTT TGT CTC TTT CCC G-3′ and 5′-CTA AGA CTA CCC CAT AAC TC-3′, and for *NtHSFA6B*, 5′-TAT TGA AGA CTA CAC CAT TGA G-3′ and 5′-CAT CCA CAT CTT CAT CTT CTT C-3′ flanked 303, 278, 165 and 159 bp transcripts, respectively.

2.3. Plant cultivation and salt stress treatment

The untransformed control clonally cultivated plantlets of *N. tabacum* (designated as WT) and *AtCPK1*, *AtCPK1-KJM4-* and *AtCPK1-KJM23*-transgenic plantlets of *N. tabacum* (CPK1-OE, KJM4-OE and KJM230OE, correspondingly) were cultivated in the glass tubes using MS/2 medium containing 10 g/L sucrose (Murashige and Skoog, 1962) in climate camera (KS-200, Russia). Conditions of cultivation were following: temperature, 24/22°C; photoperiod, 16/8 h; illumination in the day time, 3000–5000 lux; humidity, 70%; with 30-day subculture intervals. The effect of salinity stress on growth of the control WT and transgenic CPK1-OE, KJM4-OE and KJM23-OE plantlets was investigated adding 30, 60, 120, 180 and 240 mM NaCl (Panreac, Barcelona, Spain) during the 30-day period of cultivation. The plantlets inoculum for stress treatment was near 400 mg (each plantlet was weighted using an electronic balance). Samples were harvested from 30-day-old plantlets and weighed. In this work, we used three independent lines of control and each type transgenic plantlets.

To study the germination of normal and transgenic seeds, 12- and 16-well plates were used with sterile paper disks soaked in distilled water with the addition of NaCl at a concentration of 90, 120, 180, and 240 mM NaCl with and without $CaCl_2$ at a concentration of 5 and 20 mM. Seeds of WT and transgenic plants were harvested from parent plants that grew together under the same conditions. The seeds were used for analysis immediately and stored at room temperature in the dark. Conditions of germinations were following: temperature, 24/22°C; photoperiod, 16/8 h; illumination in the day time, 3000–5000 lux; humidity, 70%. Green cotyledons of all analysed tobacco lines under control conditions were observed on the 3rd day; after 14 days, the results of the experiments were photographed. Both types of salt stress treatment experiments were repeated three times.

For analysis of ROS accumulation and determination of the HSF genes expression next experiments was performed. Four weeks old clonally cultivated normal and transformed tobacco plants were transferred in the liquid medium for 24 h for adaptation; than plants samples were treated with 0 and 150 mM NaCl for 2 h and for 24 h. Plants samples from 0 (control conditions) and 150 mM NaCl (2 and 24 h NaCl) supplemented medium were used for ROS determination during initial (2h) and early (24h) stage of NaCl acclimation. For analysis of the HSF genes expression we used plants treated of 150 mM NaCl for 2 h.

2.4. Laser confocal imaging of intracellular ROS

The basis of the intracellular ROS measurement is the ability of plant cells to oxidise fluorogenic dyes to their corresponding fluorescent analogues. Monitoring of the intracellular ROS level in normal and *AtCPK*-transgenic tobacco plants was performed as described previously (Bulgakov et al., 2011). Leaves of plantlets (control, WT and transgenic, CPK1-OE, KJM4-OE and KJM23-OE) were stained with 2,7-dichlorodihydrofluorescein diacetate (H2DCF-DA, Molecular Probes, Eugene, OR, USA) at the final concentration of 50 μg/ml in liquid MS/2 for 10 min at end points of growth at 25 °C in the dark. Then, explants were washed twice and the DCF fluorescence levels inside cells were immediately collected with an Axiovert 200M LSM510 META confocal microscope (Zeiss, Germany) using an argon laser ($\lambda ex = 488$ nm; emission Ch3-LP filter 505 nm). Time-series files were acquired and recorded in the computer hard drive using LSM 510 software release 4.2 (Zeiss, Germany). Data were presented as the mean values from six separate experiments (at least 30–40 cells were analysed in each experiment). To determine ROS level, we used three independent plants clones of each variant (WT and transgenic, CPK1-OE, KJM4-OE and KJM23-OE) in three technical replicates under control and stress conditions (2 and 24 h with 150 mM NaCl).

2.5. Statistical analysis

All values were expressed as the mean ± SE using Statistica 10.0 (StatSoft Inc., USA). To determine significance, a difference of $P < 0.05$ was considered. Comparisons among multiple groups were achieved by ANOVA followed by a multiple comparison protocol, while two independent categories were compared using the Student's *t*-test. Fisher's protected least significant difference (PLSD) *post-hoc* test was employed for the inter-group comparison.

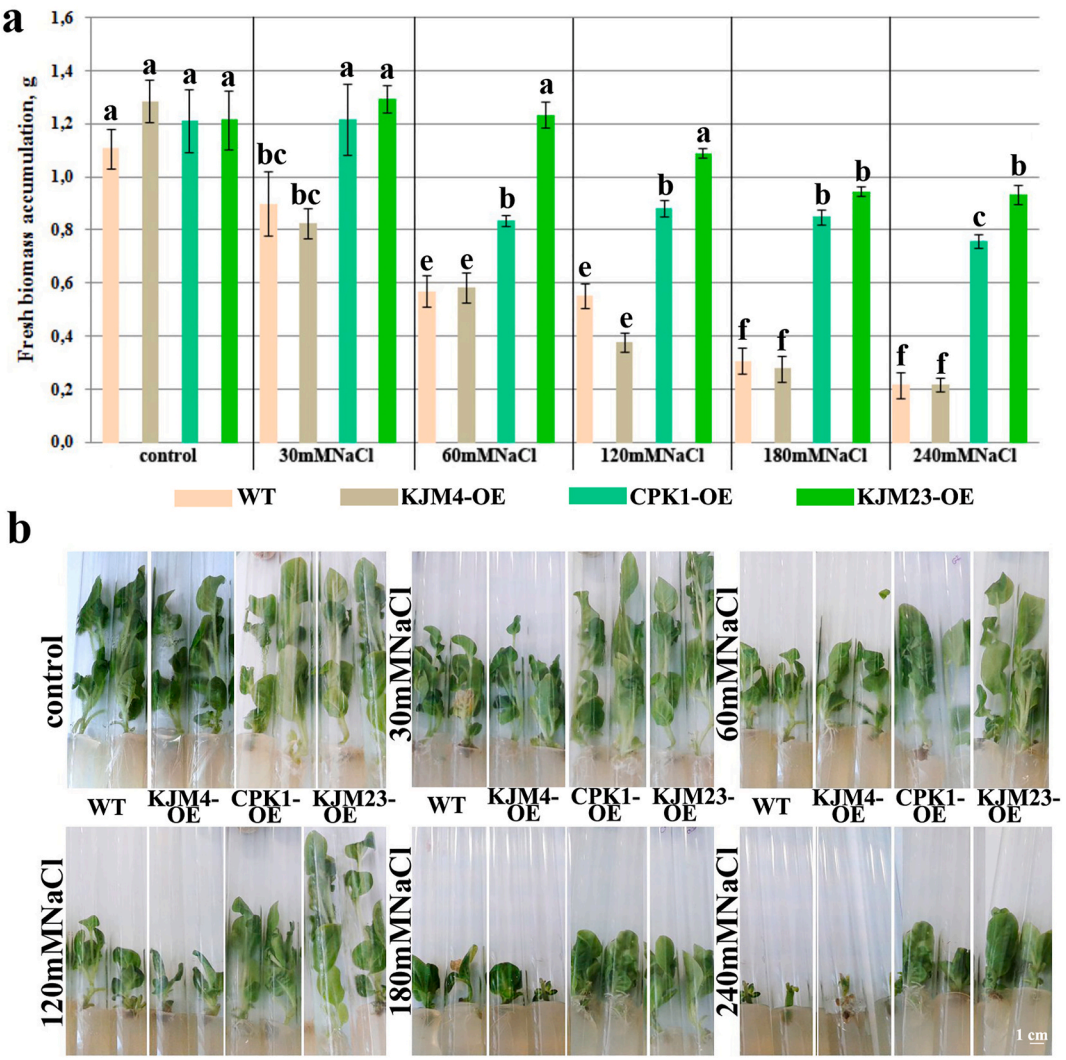

Fig. 1. Tolerance of the *N. tabacum* normal and transgenic plants to salt stress. WT, untransformed control plants; KJM4-OE, *N. tabacum* plants transformed with not active mutant form of *AtCPK1*; CPK1-OE, *N. tabacum* plants transformed with native form of *AtCPK1*; KJM23-OE, *N. tabacum* plants transformed with constitutively active mutant form of *AtCPK1*. The control and transgenic plants were clonally cultivated in the normal cultivation conditions (control) and in the presence of NaCl (30, 60, 120, 180 and 240 mM). Values of fresh biomass accumulation (**a**) are presented as means ± standard errors obtained in three separate experiments consisting of ten replicates each, different letters above the bars indicate significantly different means ($p < 0.05$), Fisher's LSD. The cultivation temperature was 24 °C; after 30 days of cultivation, plants were photographed (**b**).

3. Results

3.1. Obtaining N. tabacum transgenic plants expressing native and mutant forms of AtCPK1

Previously, we showed that *AtCPK1-Ca* (KJM23 mutation) increases the stress tolerance of *R. cordifolia* transgenic cell cultures (Veremeichik et al., 2021). In the present study, we tested whether constitutive expression of native and mutant forms of the *AtCPK1* can provide resistance to salt stress in *N. tabacum* transgenic plants. Transgenic plants were regenerated from the corresponding initial callus cultures to obtain WT and transgenic, CPK1-OE, KJM4-OE and KJM23-OE plants (Suppl. Fig. 1). We obtained ten regenerated clones of each transgene variant through resistance screening to high concentration of selective antibiotic, Km (100–200 mg/L). *AtCPK1* gene expression was analysed in these Km-resistant clones by real-time PCR. Three clones of each variant with the highest level of *AtCPK1* gene expression were screened out and clonally propagated by micropropagation.

To confirm the type of transgene expression (native, not active, or constitutively active forms of the *AtCPK1*), cDNA samples were prepared from normal and *AtCPK1*-transgenic plants (three independent clones of each variant). To verify that the cDNA was native and free of genomic DNA, RT-PCR amplification with primers corresponding to the *NtActin* gene was performed (Suppl. Fig. 2, a). Gene-specific RT-PCR analysis showed that all transformed tobacco plants expressed the *AtCPK1* gene (Suppl. Fig. 2, b). All variants obtained from transgenic plant *AtCPK1* amplicons were sequenced to confirm the type of mutation (native form of *AtCPK1* in CPK1-OE, not active and constitutively active forms of *AtCPK1* in KJM4-OE and KJM23-OE, respectively). Real-Time PCR analysis showed the same level of transgene expression in all transgenic clones (Suppl. Fig. 2, c).

Because mutation in autoinhibitory domain of the *KJM4* form led to almost total inactivation of the CPK1-KJM4 protein (Harper et al., 1994), these variants of transgenic plants were used as an additional control with functionally dead *AtCPK1*.

3.2. Tolerance to salt treatment in N. tabacum plants overexpressing native and mutant AtCPK1 forms

To confirm earlier findings of *AtCPK1* driving salt resistance (Huang

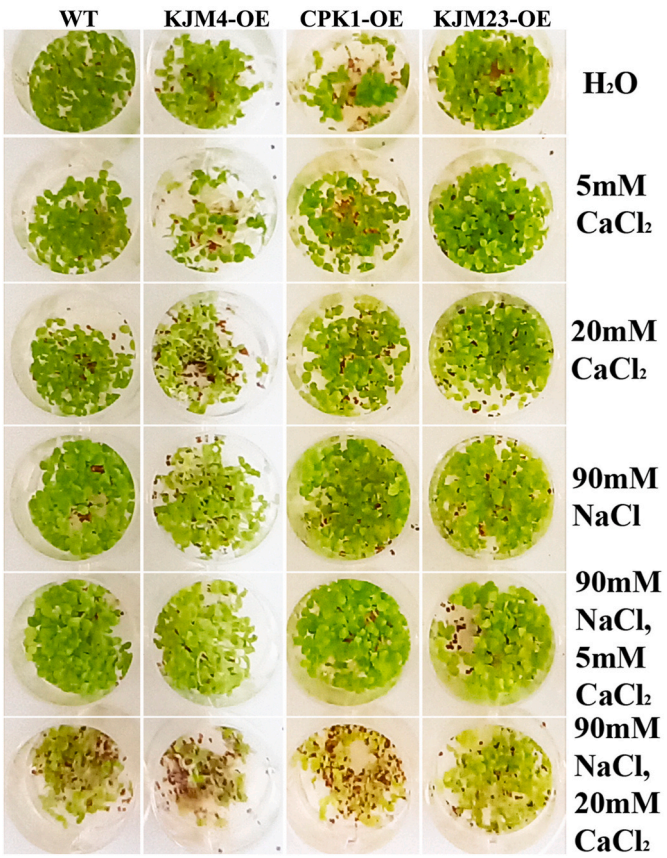

Fig. 2. Germination of the *N. tabacum* normal and transgenic plants under low salt stress with $CaCl_2$ supplementation in the concentration in 5 and 20 mM. WT, untransformed control plants; KJM4-OE, *N. tabacum* plants transformed with not active mutant form of *AtCPK1*; CPK1-OE, *N. tabacum* plants transformed with native form of *AtCPK1*; KJM23-OE, *N. tabacum* plants transformed with constitutively active mutant form of *AtCPK1*. The seeds of the control and transgenic plants were germinated in the sterile plates with paper disks soaked with distilled water (control cultivation conditions) and NaCl in the concentrations in 90 mM for 14 days with and without $CaCl_2$ (5 and 20 mM). The cultivation temperature was 24 °C.

et al., 2017; Veremeichik et al., 2021), we investigated the effect of salinity (from 30 to 240 mM NaCl) on normal and *AtCPK1* expressing tobacco plants. Growth of the control plants, determined as fresh biomass accumulation, was significant decreased (12%) by the minimum concentration of NaCl (30 mM). Increasing the NaCl concentration up to 60 and 120 mM led to 2-fold inhibition of growth in control plants. A subsequent increase of the NaCl concentration up to 180 and 240 mM almost completely inhibited the growth of WT plants (Fig. 1). The growth of CPK1-OE plants was significantly reduced by NaCl in concentrations of 60–180 mM (<25%), while 30 mM NaCl had no effect (Fig. 1, a). Growth of CPK1-OE plants treated with 240 mM NaCl was decreased more than 30% (Fig. 1, a). Under salt stress (180 and 240 mM NaCl), the height of CPK1-OE plants was significant reduced; however, total weight was compensated by thicker leaf rosettes (Fig. 1, b). Overexpression of the CPK1-KJM4 mutated form in KJM4-OE tobacco plants had no effect on the tolerance of transgenic plants to salt (Fig. 1).

Other mutations in the autoinhibitory domain of KJM23-OE led to almost total independence of Ca^{2+} availability, which caused constitutive activity of the AtCPK1-KJM23 protein. This type of mutation led to an increased salt tolerance in transgenic tobacco plants (Fig. 1). NaCl in concentration of 180 and 240 mM had a significant effect on the growth of CPK1-OE plants, while NaCl in concentrations from 30 to 120 mM had no inhibitory effect on the height and weight of CPK1-OE plants. The height of CPK1-OE plants treated with 180 and 240 mM was less than

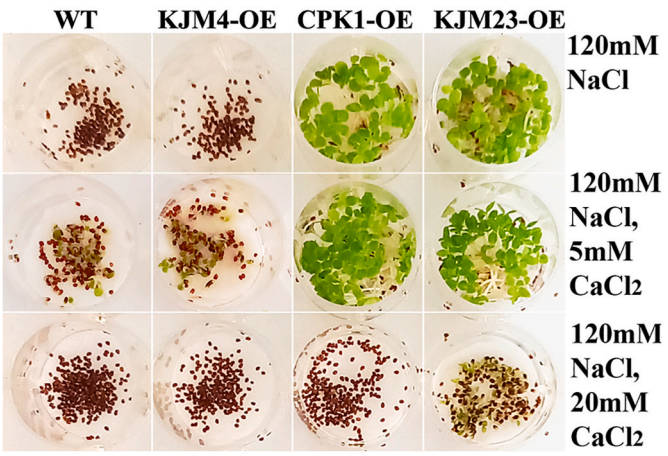

Fig. 3. Germination of the *N. tabacum* normal and transgenic plants under moderate salt stress with $CaCl_2$ supplementation in the concentration in 5 and 20 mM. WT, untransformed control plants; KJM4-OE, *N. tabacum* plants transformed with not active mutant form of *AtCPK1*; CPK1-OE, *N. tabacum* plants transformed with native form of *AtCPK1*; KJM23-OE, *N. tabacum* plants transformed with constitutively active mutant form of *AtCPK1*. The seeds of the control and transgenic plants were germinated in the sterile plates with paper disks soaked with NaCl in the concentrations in 90 mM for 14 days with and without $CaCl_2$ (5 and 20 mM). The cultivation temperature was 24 °C.

half that of those under control conditions; however, total biomass accumulation was compensated by thicker leaf rosettes, similar to observations in CPK1-OE.

3.3. Impact of Ca^{2+} supplementation on the germination of normal and AtCPK1 overexpressed N. tabacum plants under salinity treatment

In addition to prolonged growth under salt treatment, we investigated the germination of normal and transgenic seeds in the presence of NaCl. Supplementation with Ca^{2+} increases the tolerance of plants to salinity (Manishankar et al., 2018), and supplementation with 10 mM Ca^{2+} was shown to improve the growth of tobacco plants in the presence of 100 mM NaCl (Maeda et al., 2005). At the same time, concentrations of calcium more than 20 mM might be toxic for germination (Larbi et al., 2020). Concentrations of Ca^{2+} in the cultural MS/2 medium was near 2 mM. Therefore, we have performed germination assays in the absence and presence of NaCl in low (90 mM), moderate (120 mM), and high (180 and 240 mM) concentrations, with and without $CaCl_2$ at concentrations of 5 and 20 mM. Without any treatment, seeds of normal and transformed tobacco plants germinated on the 3rd day; the germination percentage in control conditions (only distilled water) was near 97% and cotyledon length was near 20 mm for all tested variants (Suppl. Fig. 3). The addition of 5 and 20 mM $CaCl_2$ did not affect seed germination. To determine the effect of NaCl alone and accompanied by $CaCl_2$, we analysed plants germinated after 14 days of incubation (Suppl. Fig.3, Figs. 2–4).

Low concentrations of NaCl (90 mM) did not affect germination time or percentage or the growth of cotyledons in tested plant lines (Suppl. Fig.3, Figs. 3 and 4). The main germination parameters did not change with the combination of 5 mM $CaCl_2$ and 90 mM NaCl. However, the combination of 90 mM NaCl and 20 mM $CaCl_2$ significantly inhibited the germination and growth of tested lines, excluding KJM23-OE (Suppl. Fig.3, Fig. 2). Moderate NaCl concentrations (120 mM) almost completely inhibited the germination of WT and KJM4-OE but did not affect CPK1-OE and KJM23-OE seed germination and cotyledons growth (Suppl. Fig.3, Fig. 2). Supplementation of 120 mM NaCl with 5 mM $CaCl_2$ significantly neutralised the effect of NaCl on WT and KJM4-OE; the germination percentage was around 50%, cotyledon length was more than two-fold less, and germination time was twice as long as that

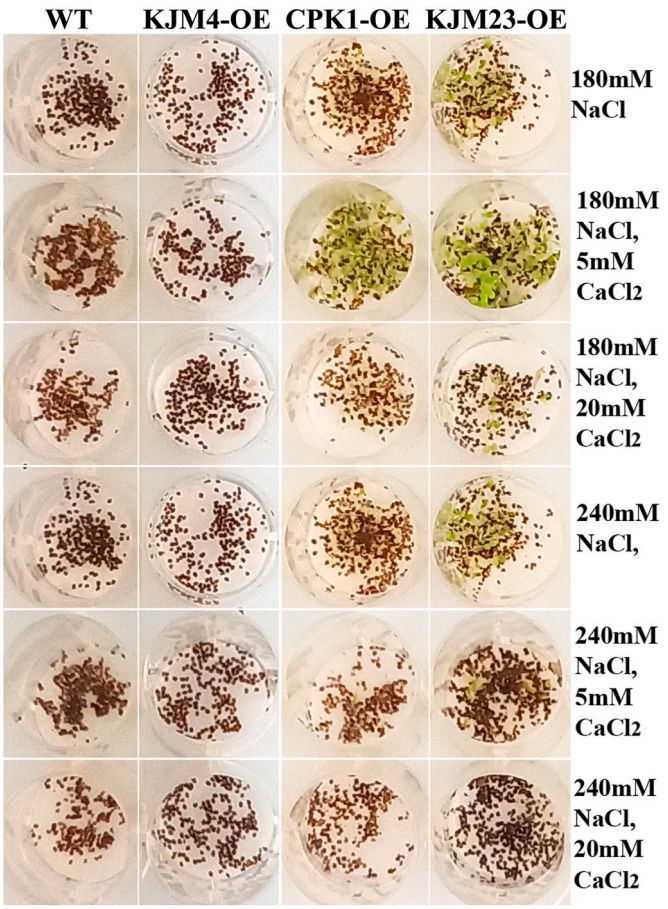

Fig. 4. Germination of the *N. tabacum* normal and transgenic plants under high salt stress with $CaCl_2$ supplementation in the concentration in 5 and 20 mM. WT, untransformed control plants; KJM4-OE, *N. tabacum* plants transformed with not active mutant form of *AtCPK1*; CPK1-OE, *N. tabacum* plants transformed with native form of *AtCPK1*; KJM23-OE, *N. tabacum* plants transformed with constitutively active mutant form of *AtCPK1*. The seeds of the control and transgenic plants were germinated in the sterile plates with paper disks soaked with NaCl in the concentrations in 180 and 240 mM for 14 days with and without $CaCl_2$. The cultivation temperature was 24 °C.

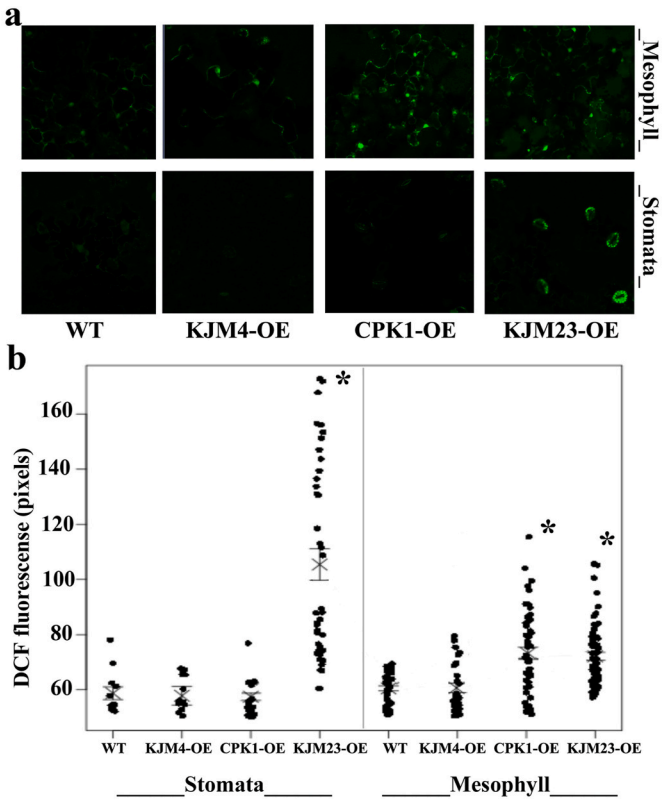

Fig. 5. DCF fluorescence (a) and abundance (b) of the intracellular ROS in the mesophyll and stomata of the *N. tabacum* and transgenic plants growth under control conditions. WT, untransformed control plants; KJM4-OE, *N. tabacum* plants transformed with not active mutant form of *AtCPK1*; CPK1-OE, *N. tabacum* plants transformed with native form of *AtCPK1*; KJM23-OE, *N. tabacum* plants transformed with constitutively active mutant form of *AtCPK1*. ROS levels presented as means ± standard errors from six independent experiments. The data are presented as mean ± SE. Asterisk above the bars indicate significantly different means between WT/KJM4-OE and CPK1-OE/KJM23-OE ($p < 0.05$), *T*-test.

under control conditions. However, supplementation of 120 mM NaCl with 20 $CaCl_2$ was highly toxic for WT, KJM4-OE, and CPK1-OE but not for KJM23-OE. The germination percentage, cotyledon length, and germination time of KJM23-OE was slightly affected, but less than two-fold (Suppl. Fig. 3 and 3).

A high NaCl concentration (180 and 240 mM) completely inhibited the germination of WT, KJM4-OE, and CPK1-OE, however KJM23-OE seeds germinated under these conditions (Suppl. Fig.3, Fig. 4). Adding $CaCl_2$ to 180 and 240 mM NaCl did not neutralise the NaCl inhibitory effect on WT and KJM4-OE. However, adding 5 mM $CaCl_2$ to 180 mM NaCl allowed CPK1-OE seed germination with a reduction in the germination percentage and cotyledons length (>2-fold) and prolonged of germination time (2-fold increase) (Suppl. Fig.3, Fig. 4). The germination percentage and cotyledon length of KJM23-OE seeds under 180 and 240 mM NaCl, with and without the addition of 5 mM $CaCl_2$, were similar and significantly affected compared to control conditions. The addition of 20 mM $CaCl_2$ to 180 mM NaCl slightly affected the germination of KJM23-OE. The addition of 20 mM $CaCl_2$ to the high NaCl concentration (240 mM) was toxic for the germination of KJM23-OE seeds too (Suppl. Fig.3, Fig. 4).

3.4. ROS accumulation in the control and AtCPK-transformed N. tabacum plants

Our earlier investigation showed that AtCPK1-Ca drove the increase in intracellular ROS in transformed callus cultures of *R. cordifolia* (Bulgakov et al., 2011; Veremeichik et al., 2021). The high content of anthraquinones in *AtCPK1-Ca* transformed *R. cordifolia* cells distorted the ROS accumulation; moreover, monitoring of ROS accumulation in full plants can give a more realistic image of ROS accumulation driven by *AtCPK1* in the mesophyll and stomata.

The dye H_2DCF-DA reacts with ROS, such as hydrogen peroxide, peroxyl radicals, and peroxynitrite. The monitoring of intracellular ROS accumulation was performed by confocal microscopy, measuring the fluorescence in single living cells of the mesophyll and stomata loaded with H_2DCF-DA. ROS accumulation in control plants, not transgenic WT, and transformed KJM4-OE plants were the same (Fig. 5, a). Overexpression of the native form of the *AtCPK1* gene led to a 1.5-fold increase compared to the control (WT and KJM4-OE) plants (Fig. 5, a). In KJM23-OE plants, a 1.2- and 1.8-fold increase of the intracellular ROS was detected compared to control plants (WT and KJM4-OE) and CPK1-OE, respectively (Fig. 5, a).

We also analysed the ROS level under salinity stress. In our previous works, we analysed the ROS level after long-term low salinity treatment (60 mM NaCl for 30 days). In the present study, we investigated the effect of high salinity (150 mM NaCl) on the ROS level in the initial (2 h) and early (24 h) stages of salt stress. The monitoring of intracellular ROS

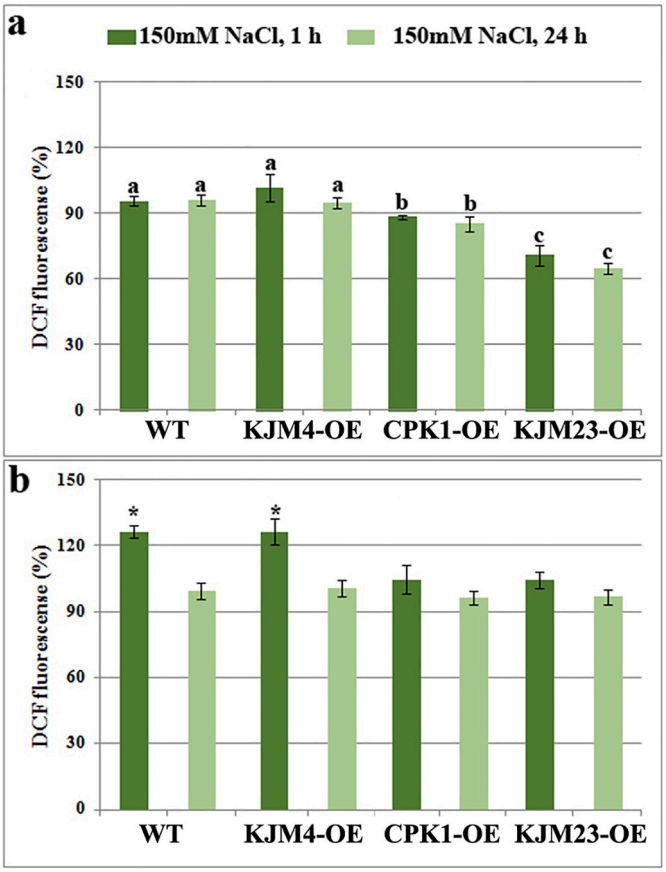

Fig. 6. Abundance of the intracellular ROS in the mesophyll (a) and stomata (b) of the *N. tabacum* normal and transgenic plants growth under control and stress (150 mM NaCl, 1 and 24 h) conditions. WT, untransformed control plants; KJM4-OE, *N. tabacum* plants transformed with not active mutant form of *AtCPK1*; CPK1-OE, *N. tabacum* plants transformed with native form of *AtCPK1*; KJM23-OE, *N. tabacum* plants transformed with constitutively active mutant form of *AtCPK1*. ROS levels presented as means ± standard errors from three independent experiments. The data are presented as mean ± SE. Different letters (a section) above the bars indicate significantly different means ($p < 0.05$), Fisher's LSD; asterisk (b section) above the bars indicate significantly different means compared to 100% fluorescence without NaCl treatment ($p < 0.05$), T-test.

accumulation in the mesophyll under salt stress conditions did not show any changes in WT and KJM4-OE plants, while CPK1-OE and KJM23-OE plants showed a significant 10 and 20% decrease, respectively, compared to WT and KJM4-OE plants (Fig. 6, a). More interesting results were obtained when the ROS level was analysed in stomata. After 2 h of salt treatment, the ROS level in WT and KJM4-OE plants was more than 20% higher compared to those in control conditions; after 24 h, it was similar to that of the control. Analysis of the ROS in stomata of CPK1-OE and KJM23-OE plants under salinity treatment did not show any increase after 2 or 24 h of treatment (Fig. 6, b).

3.5. *NtHSF gene expression in the control and AtCPK-transformed N. tabacum plants under salt stress*

ROS increased in *AtCPK1*-transformed cells of *R. cordifolia* and was accompanied by activation of ROS scavenger genes, especially *RcApx2*, a homolog of *AtApx2* (Veremeichik et al., 2021). AtApx2 is the main stress responsive antioxidant enzyme, and expression of AtApx2 was strongly regulated by HSFs under stress, including salinity treatment (Huang et al., 2016). We suggest that it is interesting to investigate the expression of the main *HSFs* under salinity and control conditions in wild-type plants and plants expressing native and mutant *AtCPK1* forms. For analysis, we chose four *NtHSFs* isoforms: *NtHSFA1*, *NtHSFA2*, *NtHSFA3,* and *NtHSFA6b* as the closest homologues of *AtHSFA1*, *AtHSFA2*, *AtHSFA3,* and *AtHSFA6b,* respectively.

Real-time PCR analysis showed that NaCl treatment increased the expression of *NtHSFA1*, *NtHSFA3,* and *NtHSFA6b* 2.3-, 19- and 6.4-fold, respectively, in WT and KJM4-OE plants. The expression of NtHSFA2 did not change under salt treatment. Overexpression of native *AtCPK1* and *AtCPK1-KJM23* led to an increase in the expression of *NtHSFA1*, *2,* and *3* and a decrease in the expression of *NtHSFA6b* in control conditions (Fig. 7). Moreover, the level of expression of *NtHSF1*, *2,* and *3* in KJM23-OE was significantly higher than that in CPK1-OE. Salt treatment did not change the level of expression of *NtHSFA1* and *2* in CPK1-OE and KJM23-OE lines but increased the level of *NtHSFA3* expression more than 30 times compared to WT and KJM4-OE under control conditions. At the same time, level of NtHSFA3 in WT and KJM4-OE under salinity increased only 20 times. Moreover, in KJM23-OE lines, the expression of *NtHSFA3* under salinity treatment was more than two-fold higher than that in WT and KJM4-OE under the same conditions. Notably, expression of *NtHSFA6b* was almost completely inhibited in CPK1-OE and KJM23-OE lines and did not change under salinity treatment, as in WT and KJM4-OE plants (Fig. 7).

4. Discussion

Since plant CPKs were first described in soybean (Harper et al., 1991), among the many CDPK genes identified in various plants, the AtCPK1 protein from *Arabidopsis* (previously termed AK1) has been used as a prototype for studying the enzymological and biochemical properties and functions of plant CPKs (Harper et al., 2004). The AtCPK1 protein is localised in peroxisomes and lipid bodies, indicating its important role in oxidative stress, lipid metabolism, and stress-defence reactions (Dammann et al., 2003; Coca and San Segundo, 2010). The *AtCPK1* gene is a positive regulator of plant responses to biotic (Valmonte et al., 2014; Delormel and Boudsocq, 2019) and abiotic stresses (Huang et al., 2017; Veremeichik et al., 2021). Our previous research showed the positive role of AtCPK1 in the regulation of phytoalexin biosynthesis (Bulgakov et al., 2011; Shkryl et al., 2011, 2016; Veremeichik et al., 2016, 2019). Biochemical analyses revealed that CPK1 plays a key role in the control of ROS generation and PCD regulation by the phosphorylation of *Arabidopsis* RBOHD and RBOHF isoforms (Gao et al., 2013) and ORE1 (Durian et al., 2020). Overexpression of the native form of AtCPK1 led to an accumulation of salicylic acid (SA) and constitutive expression of SA-regulated defence and disease resistance genes (Coca and San Segundo, 2010) and induced salt and drought tolerance (Huang et al., 2017; Veremeichik et al., 2021).

Overexpression of native *AtCPK1* in *Arabidopsis* plants improved the salt tolerance of seeds from 120 to 140 mM NaCl (Huang et al., 2017). Our previous research showed that inhibition of the junction in *AtCPK1* (*AtCPK1-KJM23* mutation) increased growth of *R. cordifolia* cells in the presents of 60 mM NaCl four times compared to control cells, while overexpression of native *AtCPK1* gave cells only a two-fold increase in salt tolerance (Veremeichik et al., 2021). In the present study, we investigated the effect of overexpressed native and mutant *AtCPK1-KJM23* forms on salinity tolerance in *Nicotiana tabacum*. Overexpression of native *AtCPK1* caused resistance in tobacco to 120 mM NaCl during germination and 180 mM NaCl during long-term growth, while the resistance of plants transformed with *AtCPK1-KJM23* increased to 240 mM NaCl during both phases of plant development. Mutation in the junction domain (*AtCPK1-KJM4*), which does not provide constitutive kinase activity, completely nullified the acquired salt tolerance up to the levels of normal plants.

In addition to increasing NaCl tolerance, the KJM23-mutation in the autoinhibitory domain of AtCPK1 provided Ca^{2+} independent NaCl tolerance and tolerance to the toxicity of the combination of high Na^{+} and Ca^{2+} concentrations in tobacco (Suppl. Fig. 3 and 3–5). The

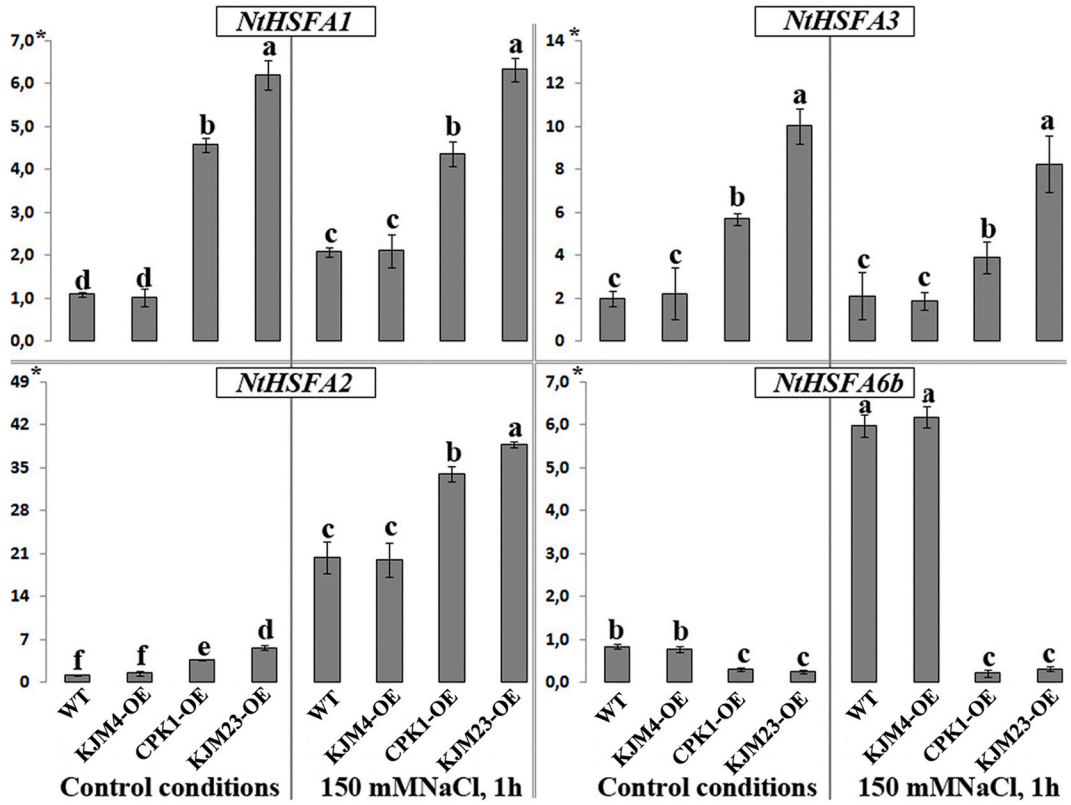

Fig. 7. Normalized expression values (*) of *NtHSF* genes in of the *N. tabacum* normal and transgenic plants growth under control conditions and salt treated (150 mM NaCl, 1 h). WT, untransformed control plants; KJM4-OE, *N. tabacum* plants transformed with not active mutant form of *AtCPK1*; CPK1-OE, *N. tabacum* plants transformed with native form of *AtCPK1*; KJM23-OE, *N. tabacum* plants transformed with constitutively active mutant form of *AtCPK1*. mRNA levels were measured by real-time RT-PCR and reported as relative expression, *NtActin* were used as reference for normalization. For this analysis, 30-day-old plants were used. The data are presented as mean ± standard error. Different letters above the bars indicate significantly different means ($p < 0.05$; Fisher's LSD).

supplementation of salinity conditions with calcium (chloride or carbonate) at low concentrations (0.3–10 mM) improved the growth of plants (Salahshoor and Kazemi, 2016; Tahjib-Ul-Arif et al., 2018; Larbi et al., 2020). It was presumed that the main role of calcium in salinity tolerance is activation of the SOS pathway, consisting of a Ca^{2+} sensor, protein kinase, and CBL–CIPK pathway (Manishankar et al., 2018). However, high concentrations of calcium are toxic for plants (Bassett, 1980; White and Broadley, 2003). In the present study, we showed that moderate concentrations of $CaCl_2$ (5 mM) successfully improved salinity tolerance of control (WT and KJM4-OE) seeds to moderate levels of NaCl (120 mM); at the same time, 20 mM $CaCl_2$ had no positive effect (Suppl. Fig.3, Fig. 4). Moreover, 20 mM $CaCl_2$ added to 90 mM NaCl significantly impaired seed germination of WT, KJM4-OE, and CPK1-OE lines. Additionally, the germination of KJM23-OE seeds was independent of $CaCl_2$ concentration. Only combinations of the highest concentrations of Na^+ and Ca^{2+} were toxic for KJM23-OE seeds. The inhibition of cotyledon growth under combinations of 120–180 mM NaCl and 20 mM $CaCl_2$ cannot be explained by increasing Cl^- concentration. High Cl^- concentrations are toxic for plants (Tester and Davenport, 2003). Despite this, in our study, the growth of control tobacco was improved in the case of 120 mM NaCl + 5 mM $CaCl_2$ then 120 mM NaCl, and growth of CPK1-OE was better in the case 120 mM NaCl + 5 mM $CaCl_2$ than 90 mM NaCl + 20 mM $CaCl_2$. This was demonstrated by the toxicity of high concentrations of Na^+ and Ca^{2+} when used together.

Previously, it was shown that the contribution of various genes to salt resistance in tobacco plants varies from 100 to 300 mM, usually with 30–50% inhibition in the experiment, while the growth of control plants was almost completely suppressed. For example, expression of the poplar *NAC13* gene in *N. tabacum* allowed plants to grow at high doses of NaCl (300 mM), with 50% growth inhibition, whereas control plants were completely inhibited (Cheng et al., 2020). Overexpression of the monodehydroascorbate reductase (*MDHAR*) gene, which is essential for ascorbic acid (AsA) recovery, increased the salt tolerance of *N. tabacum* by balancing ROS homeostasis. In this case, 100 mM NaCl stress was tested (Qi et al., 2020). Peroxiredoxins (Prxs) are a large family of antioxidant enzymes that respond to biotic and abiotic stress by decomposing ROS. A *Tamarix hispida* Prxs gene, *Th2CysPrx*, expressed in tobacco, improved the growth of tobacco plants subjected to NaCl stress (125 mM for 10 d) by lowering the ROS level and decreasing cellular damage under salt stress (Wang et al., 2020). These examples demonstrate the correlation between high salt tolerance and low levels of ROS. However, it has been repeatedly shown that AtCPK1 increases ROS accumulation (Xing et al., 2001; Bulgakov et al., 2011; Veremeichik et al., 2021). The ROS level in *AtCPK1*-expressed cells of *R. cordifolia* was not reduced under prolonged salt treatment (60 mM for 30 days), as in the control cells. However, *AtCPK1*-expressed cells with higher ROS levels were more than two-fold more tolerant to salinity (Veremeichik et al., 2021). In the present study, we clarified this inconsistency. As shown in Fig. 5, ROS accumulation in CPK1-OE and the stomata of KJM23-OE was dramatically increased compared to WT and KJM4-OE without any additional stress treatment. Under salinity stress, the ROS level in WT and KJM4-OE plants rapidly increased in stomata. The overexpression of *AtCPK1* and its mutant form *AtCPK1-KJM23* maintained ROS accumulation at the untreated level, likely protecting cells from NaCl toxicity. Moreover, at the earlier stages of NaCl treatment (1–24 h), the ROS level in the mesophyll of *AtCPK1*-expressed cells (despite mutation KJM4) was significantly decreased compared to control conditions. We suggested that high ROS levels in AtCPK1-expressed cells may be necessary for establishing salt tolerance by upregulating defence gene expression (Huang et al., 2017;

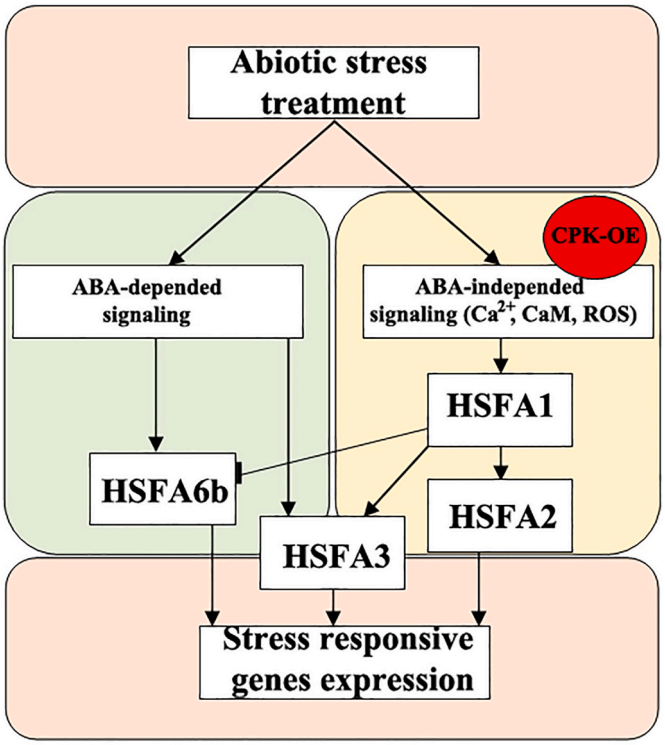

Fig. 8. A simplified model suggesting the mechanism of CPK action on *HSF* gene expression. The present model is based on a study by Huang et al. (2016), which showed that HSFA6b Arabidopsis acts as a downstream regulator of the ABA-mediated stress response. Abiotic stress (AbS) induces ABA-dependent and ABA-independent plant cell responses. ABA-independent signaling includes the Ca^{2+} (CaM, Calmodulin, and Calcium depended protein kinases) and ROS signaling systems. Under AbS, $Ca^{2+}$and ROS depended activation of the HSFA1 induces the expression of HSR genes, including the dominant factor HSFA2. HSFA3 is regulated by both ABA dependent and independent systems. HSFA6b is one of the downstream regulators of the ABA-dependent pathway. Stress responsive genes include ABA-dependent and HSR regulons, as well as OxR (oxidative stress response, including Apx2). The red circle indicates the place and suggested participation in stress response of the introduced OE CPK. (For interpretation of the references to colour in this figure legend, the reader is referred to the Web version of this article.)

Veremeichik et al., 2021), thus increasing the threshold of the cell's defence, which in turn provides increased stress tolerance.

As we previously demonstrated, overexpression of *AtCPK1* leads to activation of the ROS detoxification system. This should stabilise ROS below toxic levels and provide conditions for tolerance to stress treatments, including high salinity. Among other ROS-scavenging enzymes, Apx2 (in *Arabidopsis*) is one of the main stress-inducible isoforms, and its expression level is often used as a stress marker (Guo et al., 2016). In previous research, it was shown that *Apx2* gene expression is the most highly induced by *AtCPK1,* among other ROS-detoxifying enzymes (Huang et al., 2017; Veremeichik et al., 2021). The expression of *Apx2* is strongly regulated by HSFs (Huang et al., 2016). In the present study, we analysed the impact of overexpression of native and mutant AtCPK1 forms on the main *HSF* tobacco genes. We analysed the expression of *NtHSFA1*, *NtHSFA2*, *NtHSFA3,* and *NtHSFA6b* genes, which are homologous to *AtHSFA1*, *AtHSFA2*, *AtHSFA3,* and *AtHSFA6b,* respectively. As shown in Fig. 7, overexpression of *AtCPK1* (and its KJM23-mutant form) led to a significant (>5-fold) increase of *NtHSFA1*, *NtHSFA2*, and *NtHSFA3* and decrease (>2-fold) of *NtHSFA6b*. The expression of *HSFA1* is regulated through Ca^{2+} signalling and dependent on the ROS level, whereas the expression of *HSFA6b* is ABA-regulated and Ca^{2+} and ROS independent. HSFA1 is a regulator of *HSF* expression, regulating HSFA2 and HSFA3 positively and HSFA6b negatively (Huang et al., 2016). Salinity treatment increased the expression of *NtHSFA1*, *NtHSFA2,* and *NtHSFA6b* in wild-type tobacco plants; the most salt-activated was *NtHSFA2*. The overexpression of *AtCPK1* (native and KJM23-mutant) led to a salinity-induced increase in *NtHSFA2*; notably, in WT and KJM4-OE plants expression of this HSF isoforms was induced under salinity too, but significantly less, than in CPK1-OE and KJM23-OE plants. In Fig. 8, we proposed a putative possible model for the involvement of CPK1 in HSF-dependent regulation of stress-dependent genes. To our knowledge, this is the first indication that the overexpression of plant CDPKs can affect the expression of plant *HSF* genes. This effect may be linked with salt tolerance. Moreover, we first described the effect of mutations in the autoinhibitory domain on the ability of the recombinant CDPK to activate the response to abiotic stress in plants. Substitution of only six amino acid residues in the middle or four at the end of the 35 aa Junction can enhance or completely disable the CDPK effect, and the distance between these key substitutions is just nine amino acid residues. Based on the results of the present and previous research, we suggest the autoinhibitory domains of CDPKs are promising targets for manipulation in the field of genetic engineering in plants.

Author contributions section

G.N. Veremeichik, Y.N. Shkryl, V.P. Bulgakov conceived and planned the experiments, wrote the manuscript.

G.N. Veremeichik, S.A. Silantieva, E.V. Brodovskaya, plant transformation and cultivation, stress treatment experiments.

G.N. Veremeichik, Real Time PCR.

T.Y. Gorpenchenko, M.S. Yatsunskaya, confocal microscopy.

Declaration of competing interest

The authors declare that they have no known competing financial interests or personal relationships that could have appeared to influence the work reported in this paper.

Acknowledgments

Financial support was provided by the Russian Science Foundation, Grant no. 20-16-00016 (V.P. Bulgakov). The analyses described in this work were performed using equipment from the Instrumental Centre for Biotechnology and Gene Engineering at the Federal Scientific Centre of East Asia Terrestrial Biodiversity of the Far East Branch of the Russian Academy of Sciences.

Appendix A. Supplementary data

Supplementary data to this article can be found online at https://doi.org/10.1016/j.plaphy.2021.05.026.

References

Almadanim, M.C., Goncalves, N.M., Rosa, M.T.G., Alexandre, B.M., Cordeiro, A.M., Rodrigues, M., Saibo, N.J.M., Soares, C.M., Romao, C.V., Oliveira, M.M., Abreu, I.A., 2017. The rice cold-responsive calcium-dependent protein kinase *OsCPK17* is regulated by alternative splicing and post-translational modifications. Biochim. Biophys. Acta Mol. Cell 1865 (2), 231–246. https://doi.org/10.1016/j.bbamcr.2017.10.010.

Bassett, P.A., 1980. The effect of soil salinity and calcium levels on the growth of *Bromus mollis* in the Camargue, France. Oikos 35 (3), 353–358. https://doi.org/10.2307/3544651.

Bender, K.W., Zielinski, R.E., Huber, S.C., 2018. Revisiting paradigms of Ca^{2+} signaling protein kinase regulation in plants. Biochem. J. 475, 207–223. https://doi.org/10.1042/BCJ20170022.

Boudsocq, M., Droillard, M.J., Regad, L., Laurière, C., 2012. Characterization of *Arabidopsis* calcium-dependent protein kinases: activated or not by calcium? Biochem. J. 447 (2), 291–299. https://doi.org/10.1042/bj20112072.

Bulgakov, V.P., Gorpenchenko, T.Y., Shkryl, Y.N., Veremeichik, G.N., Mischenko, N.P., Avramenko, T.V., Fedoreyev, S.A., Zhuravlev, Y.N., 2011. CDPK-driven changes in the intracellular ROS level and plant secondary metabolism. Bioeng. Bugs 2 (6), 327–330. https://doi.org/10.4161/bbug.2.6.16803.

Chandran, V., Stollar, E.J., Lindorff-Larsen, K., Harper, J.F., Chazin, W.J., Dobson, C.M., Luisi, B.F., Christodoulou, J., 2006. Structure of the regulatory apparatus of a calcium-dependent protein kinase (CDPK): a novel mode of calmodulin-target recognition. J. Mol. Biol. 357, 400–410. https://doi.org/10.1016/j.jmb.2005.11.093.

Cheng, Z., Zhang, X., Zhao, K., Zhou, B., Jiang, T., 2020. Ectopic expression of a poplar gene *NAC13* confers enhanced tolerance to salinity stress in transgenic *Nicotiana tabacum*. J. Plant Res. 133 (5), 727–737. https://doi.org/10.1007/s10265-020-01213-z.

Coca, M., San Segundo, B., 2010. *AtCPK1* calcium-dependent protein kinase mediates pathogen resistance in *Arabidopsis*. Plant J. 63, 526–540. https://doi.org/10.1111/j.1365-313X.2010.04255.

Dammann, C., Ichida, A., Hong, B., Romanowsky, S.M., Hrabak, E.M., Harmon, A.C., Pickard, B.G., Harper, J.F., 2003. Subcellular targeting of nine calcium-dependent protein kinase isoforms from *Arabidopsis*. Plant Physiol. 132 (4), 1840–1848. https://doi.org/10.1104/pp.103.020008.

DeFalco, T.A., Bender, K.W., Snedden, W.A., 2010. Breaking the code: Ca^{2+} sensors in plant signalling. Biochem. J. 425, 27–40. https://doi.org/10.1042/BJ20091147.

Delormel, T.Y., Boudsocq, M., 2019. Properties and functions of calcium-dependent protein kinases and their relatives in *Arabidopsis thaliana*. New Phytol. 224, 585–604. https://doi.org/10.1111/nph.16088.

Durian, G., Sedaghatmehr, M., Matallana-Ramirez, L., Schilling, S.M., Schaepe, S., Guerra, T., Herde, M., Witte, C., Mueller-Roeber, B., Schulze, W.X., Balazadeh, S., Romeis, T., 2020. Calcium-dependent protein Kinase CPK1 controls cell death by *in vivo* phosphorylation of senescence master regulator ORE1. Plant Cell 32 (5), 1610–1625. https://doi.org/10.1105/tpc.19.00810.

Edel, K.H., Kudla, J., 2015. Increasing complexity and versatility: how the calcium signaling toolkit was shaped during plant land colonization. Cell Calcium 57 (3), 231–246. https://doi.org/10.1016/j.ceca.2014.10.013.

Gao, X., Chen, X., Lin, W., Chen, S., Lu, D., Niu, Y., Li, L., Cheng, C., McCormack, M., Sheen, J., Shan, L., He, P., 2013. Bifurcation of *Arabidopsis* NLR immune signaling via Ca^{2+}-dependent protein kinases. PLoS Pathog. 9 (1), e1003127 https://doi.org/10.1371/journal.ppat.1003127.

Guo, M., Liu, J., Ma, X., Luo, D., Gong, Z., Lu, M., 2016. The plant heat stress transcription factors (HSFs): structure, regulation, and function in response to abiotic stresses. Front. Plant Sci. 7, 114. https://doi.org/10.3389/fpls.2016.00114.

Harper, J.F., Sussman, M.R., Schaller, G.E., Putnam-Evans, C., Charbonneau, H., Harmon, A.C., 1991. A calcium-dependent protein kinase with a regulatory domain similar to calmodulin. Science 252 (5008), 951–954. https://doi.org/10.1126/science.1852075.

Harper, J.F., Huang, J.F., Lloyd, S.J., 1994. Genetic identification of an autoinhibitor in CDPK, a protein kinase with a calmodulin-like domain. Biochemistry 33, 7267–7277. https://doi.org/10.1021/bi00189a031.

Harmon, AC, Yoo, B-C, McCaffery, C, 1994. Pseudosubstrate inhibition of CDPK, a protein kinase with a calmodulin-like domain. Biochemistry 33, 7278–7287. https://doi.org/10.1021/bi00189a032.

Harper, J.F., Breton, G., Harmon, A., 2004. Decoding Ca^{2+} signals through plant protein kinases. Annu. Rev. Plant Biol. 55 (1), 263–288. https://doi.org/10.1146/annurev.arplant.55.031903.141627.

Horsch, R.B., Fry, J.E., Hoffmann, N.L., Eichholtz, D., Rogers, S.G., Fraley, R.T., 1985. A simple and general method for transferring genes into plants. Science 227, 1229–1231. https://doi.org/10.1126/science.227.4691.1229.

Hrabak, E.M., Chan, C.W.M., Gribskov, M., Harper, J.F., Choi, J.H., Halford, N., Kudla, J., Luan, S., Nimmo, H.G., Sussman, M.R., Thomas, M., Walker-Simmons, K., Zhu, J., Harmon, A.C., 2003. The *Arabidopsis* CDPK-SnRK superfamily of protein kinases. Plant Physiol. 132 (2), 666–680. https://doi.org/10.1104/pp.102.011999.

Huang, J., Teyton, L., Harper, J.F., 1996. Activation of a Ca^{2+}-dependent protein kinase involves intramolecular binding of a calmodulin-like regulatory domain. Biochemistry 35 (40), 13222–13230. https://doi.org/10.1021/bi960498a.

Huang, Y., Niu, C., Yang, C., Jinn, T., 2016. The heat stress factor HSFA6b connects ABA signaling and ABA-mediated heat responses. Plant Physiol. 172 (2), 1182–1199. https://doi.org/10.1104/pp.16.00860.

Huang, K., Peng, L., Liu, Y., Yao, R., Liu, Z., Li, X., Yang, Y., Wang, J., 2017. Calcium-dependent protein kinase *AtCPK1* plays a positive role in salt/drought-stress response. Biochem. Biophys. Res. Commun. 498 (1), 92–98. https://doi.org/10.1016/j.bbrc.2017.11.175.

Kudla, J., Batistic, O., Hashimoto, K., 2010. Calcium signals: the lead currency of plant information processing. Plant Cell 22, 541–563. https://doi.org/10.1105/tpc.109.072686.

Kudla, J., Becker, D., Grill, E., Hedrich, R., Hippler, M., Kummer, U., Parniske, M., Romeis, T., Schumacher, K., 2018. Advances and current challenges in calcium signaling. New Phytol. 218, 414–431. https://doi.org/10.1111/nph.14966.

Larbi, A., Kchaou, H., Gaaliche, B., Gargouri, K., Boulal, H., Moralese, F., 2020. Supplementary potassium and calcium improves salt tolerance in olive plants. Sci. Hortic. 260, 108912. https://doi.org/10.1016/j.scienta.2019.108912.

Liu, H., Che, Z., Zeng, X., Zhou, X., Sitoe, H.M., Wang, H., Yu, D., 2016. Genome-wide analysis of calcium-dependent protein kinases and their expression patterns in response to herbivore and wounding stresses in soybean. Funct. Integr. Genom. 16 (5), 481–493. https://doi.org/10.1007/s10142-016-0498-8.

Maeda, Y., Yoshiba, M., Tadano, T., 2005. Comparison of Ca effect on the salt tolerance of suspension cells and intact plants of tobacco (*Nicotiana tabucum* L., cv. bright yellow-2). Soil Sci. Plant Nutr. 51 (4), 485–490. https://doi.org/10.1111/j.1747-0765.2005.tb00056.x.

Manishankar, P., Wang, N., Kuster, P., Alatar, A.A., Kudla, J., 2018. Calcium signaling during salt stress and in the regulation of ion homeostasis. J. Exp. Bot. 69 (17), 4215–4226. https://doi.org/10.1093/jxb/ery201.

McCarron, J.G., Chalmers, S., Olson, M.L., Girkin, J.M., 2012. Subplasma membrane Ca^{2+} signals. IUBMB Life 64 (7), 573–585. https://doi.org/10.1002/iub.1032.

Murashige, T., Skoog, F., 1962. A revised medium for rapid growth and bioassays with tobacco tissue culture. Physiol. Plantarum 15, 473–497. https://doi.org/10.1111/j.1399-3054.1962.tb08052.x.

Qi, Q., Yanyan, D., Yuanlin, L., Kunzhi, L., Huini, X., Xudong, S., 2020. Overexpression of *SlMDHAR* in transgenic tobacco increased salt stress tolerance involving S-nitrosylation regulation. Plant Sci. 299 https://doi.org/10.1016/j.plantsci.2020.110609.

Raichaudhuri, A., Bhattacharyya, R., Chaudhuri, S., Chakrabarti, P., Dasgupta, M., 2006. Domain analysis of a groundnut calcium-dependent protein kinase: nuclear localization sequence in the junction domain is coupled with nonconsensus calcium binding domains. J. Biol. Chem. 281 (15), 10399–10409. https://doi:10.1074/jbc.M511001200.

Salahshoor, F., Kazemi, F., 2016. Effect of calcium on reducing salt stress in seed germination and early growth stage of *Festuca ovina* L. Plant Soil Environ. 62 (10), 460–466. https://doi.org/10.17221/319/2016-PSE.

Shkryl, Y.N., Veremeichik, G.N., Bulgakov, V.P., Tchernoded, G.K., Mischenko, N.P., Fedoreyev, S.A., Zhuravlev, Y.N., 2008. Individual and combined effects of the *rolA, B*, and *C* genes on anthraquinone production in *Rubia cordifolia* transformed calli. Biotechnol. Bioeng. 100 (1), 118–125. https://doi.org/10.1002/bit.21727.

Shkryl, Y.N., Veremeichik, G.N., Bulgakov, V.P., Zhuravlev, Y.N., 2011. Induction of anthraquinone biosynthesis in *Rubia cordifolia* cells by heterologous expression of a calcium-dependent protein kinase gene. Biotechnol. Bioeng. 108 (7), 1734–1738. https://doi.org/10.1002/bit.23077.

Shkryl, YN, Veremeichik, GN, Kamenev, DG, Gorpenchenko, TY, Yugay, YA, Mashtalyar, DV, Nepomnyaschiy, AV, Avramenko, TV, Karabtsov, AA, Ivanov, VV, Bulgakov, VP, Gnedenkov, SV, Kulchin, YN, Zhuravlev, YN, 2018. Green synthesis of silver nanoparticles using transgenic *Nicotiana tabacum* callus culture expressing silicatein gene from marine sponge *Latrunculia oparinae*. Artif Cells Nanomed Biotechnol 46 (8), 1646–1658. https://doi.org/10.1080/21691401.2017.1388248.

Shkryl, Y.N., Veremeichik, G.N., Makhazen, D.S., Silantieva, S.A., Mishchenko, N.P., Vasileva, E.S., Fedoreyev, S.A., Bulgakov, V.P., 2016. Increase of anthraquinone content in *Rubia cordifolia* cells transformed by native and constitutively active forms of the *AtCPK1* gene. Plant Cell Rep. 9 (35) https://doi.org/10.1007/s00299-016-2005-z, 19017-1916.

Sun, H., Sun, X., Wang, H., Ma, X., 2020. Advances in salt tolerance molecular mechanism in tobacco plants. Hereditas 157 (1), 5. https://doi.org/10.1186/s41065-020-00118-0.

Tahjib-Ul-Arif, Md, Roy, P.R., Mamun, Sohag AAl, Afrin, S., Rady, M.M., Hossain, M.A., 2018. Exogenous calcium supplementation improves salinity tolerance in BRRI Dhan28; a salt-susceptible high-yielding *Oryza Sativa* cultivar. J. Crop Sci. Biotech. 21 (4), 383–394. https://doi.org/10.1007/s12892-018-0098-0.

Tester, M., Davenport, R., 2003. Na^+ tolerance and Na^+ transport in higher plants. Ann. Bot. 91, 503–527. https://doi.org/10.1093/aob/mcg058.

Valmonte, G.R., Arthur, K., Higgins, C.M., MacDiarmid, R.M., 2014. Calcium-dependent protein kinases in plants: evolution, expression and function. Plant Cell Physiol. 55 (3), 551–569. https://doi.org/10.1093/pcp/pct200.

Veremeichik, G.N., Grigorchuk, V.P., Shkryl, Y.N., Bulgakov, D.V., Silantieva, S.A., Bulgakov, V.P., 2016. Induction of resveratrol biosynthesis in *Vitis amurensis* cells by heterologous expression of the *Arabidopsis* constitutively active, Ca^{2+}-independent form of the *AtCPK1* gene. Process Biochem. 54, 144–155. https://doi.org/10.1016/j.procbio.2016.12.026.

Veremeichik, G.N., Grigorchuk, V.P., Silanteva, S.A., Shkryl, Y.N., Bulgakov, D.V., Brodovskaya, E.V., Bulgakov, V.P., 2019. Increase in isoflavonoid content in *Glycine max* cells transformed by the constitutively active Ca^{2+}independent form of the *AtCPK1* gene. Phytochemistry 157, 111–120. https://doi.org/10.1016/j.phytochem.2018.10.023.

Veremeichik, G.N., Shkry, Y.N., Gorpenchenko, T.Y., Silantieva, S.A., Avramenko, T.V., Brodovskaya, E.V., Bulgakov, V.P., 2021. Inactivation of the auto-inhibitory domain in *Arabidopsis AtCPK1* leads to increased salt, cold and heat tolerance in the *AtCPK1*-transformed *Rubia cordifolia* L cell cultures. Plant Physiol. Biochem. 159, 372–382. https://doi.org/10.1016/j.plaphy.2020.12.031.

Wang, Y., Liu, Z., Wang, P., Jiang, B., Lei, X., Wu, J., Dong, W., Gao, C., 2020. A 2-Cys peroxiredoxin gene from *Tamarix hispida* improved salt stress tolerance in plants. BMC Plant Biol. 20 (1), 360. https://doi.org/10.1186/s12870-020-02562-6.

Watillon, B., Kettmann, R., Boxus, P., Burny, A.R., 1993. Communication a calcium/calmodulin-binding serine/threonine protein kinase homologous to the mammalian type calcium/calmodulin-dependent protein kinase 1s expressed in plant cells. Plant Physiol. 101 (4), 1381–1384. https://doi.org/10.1104/pp.101.4.1381.

Wernimont, A.K., Amani, M., Qiu, W., Pizarro, J.C., Artz, J.D., Lin, Y., Lew, J., Hutchinson, A., Hui, R., 2011. Structures of parasitic CDPK domains point to a common mechanism of activation. Proteins 79 (3), 803–820. https://doi.org/10.1002/prot.22919.

White, P.J., Broadley, M.R., 2003. Calcium in plants. Ann. Bot. 92 (4), 487–511. https://doi.org/10.1093/aob/mcg164.

Xing, T., Wang, X.-J., Malk, K., Mikl, B., 2001. Ectopic expression of an *Arabidopsis* calmodulin-like domain protein kinase-enhanced NADPH oxidase activity and oxidative burst in tomato protoplasts. Mol. Plant Microbe Interact. 14 (10), 1261–1264. https://doi.org/10.1094/MPMI.2001.14.10.1261.

Yoo, B., Harmon, A.C., 1996. Intramolecular binding contributes to the activation of CDPK, a protein kinase with a calmodulin-like domain. Biochemistry 35 (37), 12029–12037. https://doi.org/10.1021/bi9606612.